WestVirginiaUniversity
THE RESEARCH REPOSITORY @ WVU

Faculty Scholarship

2007

Blockade Of Tumor Necrosis Factor-Induced Bid Cleavage By Caspase-Resistant Rb

XiaoDong Huang

Anja Masselli

Steven M. Frisch

Irina C. Hunton

Yong Jiang

See next page for additional authors

Follow this and additional works at: https://researchrepository.wvu.edu/faculty_publications

Authors

XiaoDong Huang, Anja Masselli, Steven M. Frisch, Irina C. Hunton, Yong Jiang, and Jean Y. J. Wang

Blockade of Tumor Necrosis Factor-induced Bid Cleavage by Caspase-resistant Rb[*][S]

XiaoDong Huang[‡§], Anja Masselli[§], Steven M. Frisch[¶], Irina C. Hunton[§], Yong Jiang[§], and Jean Y. J. Wang[‡§||1]

From the ‡Division of Biological Sciences, §Moores Cancer Center, ||Division of Hematology/Oncology, Department of Medicine, University of California, San Diego, La Jolla, California 92093-0820 and the ¶Mary Babb Randolph Cancer Center and Department of Biochemistry, West Virginia University, Morgantown, West Virginia 26506

Tumor necrosis factor-α (TNF) activates caspase-8 to cleave effector caspases or Bid, resulting in type-1 or type-2 apoptosis, respectively. We show here that TNF also induces caspase-8-dependent C-terminal cleavage of the retinoblastoma protein (Rb). Interestingly, fibroblasts from $Rb^{MI/MI}$ mice, in which the C-terminal caspase cleavage site is mutated, exhibit a defect in Bid cleavage despite caspase-8 activation. Recent results suggest that TNF receptor endocytosis is required for the activation of caspase-8. Consistent with this notion, inhibition of V-ATPase, which plays an essential role in acidification and degradation of endosomes, specifically restores Bid cleavage in $Rb^{MI/MI}$ cells. Inhibition of V-ATPase sensitizes $Rb^{MI/MI}$ but not wild-type fibroblasts to TNF-induced apoptosis and stimulates inflammation-associated colonic apoptosis in $Rb^{MI/MI}$ but not wild-type mice. These results suggest that Rb cleavage is required for Bid cleavage in TNF-induced type-2 apoptosis, and this requirement can be supplanted by the inhibition of V-ATPase.

Tumor necrosis factor-α (TNF)[2] is an inflammatory cytokine that orchestrates the systemic responses to infections and injuries. Discovered as an inducer of tumor necrosis, TNF also promotes tumor development, particularly under conditions of chronic inflammation (1–3). The tumor-promoting activity of TNF is mediated through its activation of the NF-κB pathway, which stimulates the production of cytokines, chemokines, and apoptotic inhibitors (4, 5). Nonetheless, the type-1 TNF receptor (TNFR1) contains a death domain (DD) that can induce the assembly of death-inducing signaling complex (DISC) to activate the initiator caspase-8, leading to the induction of apoptosis (6, 7). TNFR1 also activates programmed necrosis that is independent of caspase activity but mediated by reactive oxygen species (8–10). The prodeath function of TNF is observed when the NF-κB pathway is inactivated. In *ex vivo* experiments, cycloheximide (CHX) is routinely used to divert TNF signal toward death by blocking the expression of NF-κB-induced genes, such as FLIP and mitochondrial superoxide dismutase, that prevent the activation of caspase-8 and the generation of reactive oxygen species, respectively (11, 12). In cells defective in the NF-κB pathway, TNF alone (without CHX) is sufficient to induce cell death (13, 14). In mice, TNF- and TNFR1-dependent cell death is observed in a variety of mouse tissues under conditions of acute inflammation (2, 5, 15). The molecular mechanisms that govern the survival *versus* the death response to TNF are likely to be complex and have not been fully elucidated.

An important clue to how TNF differentially activates NF-κB or caspase-8 has come from recent studies showing that TNFR1 endocytosis is a prerequisite for DISC assembly (16, 17). In the plasma membrane, activated TNFR1 is capable of stimulating the NF-κB pathway, but it does not associate with FADD or caspase-8 (18, 19). By contrast, two other DD receptors (*i.e.* FAS/CD95 and DR5) do assemble DISC at the plasma membrane when activated by FAS ligand or TRAIL, respectively (19). In experiments conducted with a human fibrosarcoma cell line (HT1080) that expresses a degradation-resistant IκB-α to divert TNF signal toward caspase-8, Micheau and Tschopp (18) detected a cytosolic DISC complex containing TRADD, FADD, and caspase-8 but free of TNFR1. Subsequent studies conducted with human U937 and mouse 3T3 cells detected TNFR1-associated TRADD-FADD-caspase-8 complex in the endosomal fraction (16). Together, these results suggest that TNFR1 endocytosis and the release of DISC from the receptor-endosome may play a role in determining the cellular response to TNF.

The retinoblastoma susceptibility gene product, Rb, is a nuclear scaffolding protein with multiple protein-binding pockets (20–23). Rb inhibits the transcription of E2F-regulated genes to block cell cycle progression. Because E2F also stimulates the expression of apoptotic factors, such as caspases and Apaf-1, inhibition of E2F by Rb confers apoptotic resistance in growth-arrested cells (24). Upon stimulation with mitogenic factors, Rb is inactivated through phosphorylation by cyclin-dependent kinases to promote cell cycle entry and S-phase progression (25). Upon exposure to death stimuli, Rb is cleaved by caspase at a predominant site, DEAD[886]G[887], near the C termi-

[2] The abbreviations used are: TNF, tumor necrosis factor-α; TNFR1, type-1 receptor for TNF; MI, mutated at the ICE-site; DISC, death-inducing signaling complex; CHX, cycloheximide; DSS, dextran sulfate sodium; DD, death domain; MEF, mouse embryo fibroblast; hTNF, human TNF; mTNF, mouse TNF; TUNEL, terminal dUTP nick-end labeling; PIPES, 1,4-piperazinediethanesulfonic acid; CHAPS, 3-[(3-cholamidopropyl)dimethylammonio]-1-propanesulfonic acid; AMC, 7-amido-4-methylcoumarin; AFC, 7-amino-4-trifluoromethylcoumarin; fmk, fluoromethyl ketone; V-ATPase, vacuolar ATPase; siRNA small interfering RNA; FITC, fluorescein isothiocyanate; Baf, bafilomycin A1; FCCP, carbonyl cyanide 4-(trifluoromethoxy)phenylhydrazone; 3-MA, 3-methyladenine.

nus of the protein (26–28). Cleavage at this site generates a large fragment of Rb (RbΔI) that retains E2F-binding and transcription repression functions (26, 27, 29). Thus, the C-terminal cleavage does not interfere with the antiproliferative activity of Rb. We have mutated this C-terminal caspase cleavage site to DEAA[886]E[887] in the mouse *Rb* gene to create the *Rb-MI* allele (30). The *Rb-MI* allele confers resistance to inflammation-induced apoptosis in the mouse intestine, which is dependent on TNF (30). The *Rb-MI* allele also confers resistance to TNF-induced apoptosis in explanted thymocytes and in fibroblasts derived from the mouse embryos (30, 31). Interestingly, however, *Rb-MI* does not protect fibroblasts from apoptosis induced by TRAIL[3]; nor is it protective of hepatocyte apoptosis induced by the ligation of FAS receptor.[4]

Death receptors, such as FAS and TNFR1, stimulate apoptosis through two pathways, both activated by caspase-8 (4, 32). In the type-1 pathway, initiator caspase-8 directly cleaves and activates effector caspases to induce apoptosis (33). In the type-2 pathway, initiator caspase-8 cleaves Bid, and the resulting tBid induces mitochondria outer membrane permeability to cause the release of proapoptotic factors, leading to the activation of apoptosome and caspase-9 (33, 34). We have previously shown that TNFR1-induced cytochrome *c* release is defective in *Rb-MI* fibroblasts (30). In pursuing the mechanism underlying this defect, we have discovered that inhibition of vacuolar ATPase can restore the TNFR1-induced type-2 apoptotic pathway in *Rb-MI* cells.

The vacuolar ATPase (V-ATPase) is a proton pump that is conserved in eukaryotic cells (35, 36). Composed of a soluble V_1 complex that hydrolyzes ATP and an integral membrane V_0 complex that forms the proton channel, V-ATPase couples ATP hydrolysis to the translocation of protons from the cytosol to the lumen of late endosomes, multivesicular bodies, and lysosomes (35, 37). V-ATPase-dependent luminal acidification provides the necessary condition for lysosomal degradative enzymes to perform their functions. Moreover, acidification is also required for endosomal trafficking (37, 38), best demonstrated by a recent report that V-ATPase allows the recruitment of Arf6 and ARNO to the endosomal membrane for sorting to the multivesicular body and lysosome (39). We show here that TNFR1 activates the 43-kDa endosomal caspase-8 in *Rb-MI* cells, but Bid is not cleaved. However, Bid cleavage is rescued either by the knockdown of Rb-MI or by the inhibition of V-ATPase.

EXPERIMENTAL PROCEDURES

Cell Culture—Fibroblasts derived from $Rb^{+/+}$ (*Rb-wt*) and $Rb^{MI/MI}$ (*Rb-MI*) mouse embryos were immortalized through the 3T3 passage protocol. The *Caspase-8*$^{-/-}$ and *Caspase-8*$^{+/+}$ MEFs (40) were gifts from Dr. David Wallach (Weizmann Institute, Israel). MEFs were cultured in Dulbecco's modified Eagle's medium containing 10% fetal bovine serum, penicillin/streptomycin, and 0.05% β-mercaptoethanol. Cells were routinely treated with 10 ng/ml recombinant human TNF (hTNF) plus 2.5 μg/ml CHX for 5 h at 37 °C unless noted otherwise.

Antibodies and Chemicals—Rb antibodies used are rabbit anti-Rb (851) raised against the C-terminal fragment (residues 768–928) of Rb (20) and anti-Rb from Pharmingen (554136); rat anti-caspase-8 (1G12) and rat anti-FADD (12E7) were from Alexis Biochemicals; rabbit anti-Smac was from Chemicon; goat anti-Bid and rabbit anti-Cox-IV were from Biovision; goat-anti-ATP6V1B1 (N-20), rabbit-anti-Mcl-1 (S-19), and rabbit anti-TRADD (H-278) were from Santa Cruz Biotechnology, Inc. (Santa Cruz, CA); rabbit anti-phospho-c-Jun, mouse anti-cleaved caspase-3 (5A1), and rabbit anti-PARP1 were from Cell Signaling Technology; mouse anti-cytochrome *c* antibody was from BD Biosciences; biotin-VAD-fmk was from Kamiya; the caspase-8 fluorometric assay kit was from Biovision; the caspase-3 fluorometric assay kit was from Molecular Probes; the TUNEL staining kit was obtained from BD Biosciences; recombinant human and mouse TNF were from R & D Systems; MG-132 and cathepsin inhibitor benzyloxycarbonyl-YY-fmk were from Calbiochem; and bafilomycin A1, concanamycin A, and carbonyl cyanide 4-(trifluoromethoxy)phenylhydrazone (FCCP) were from Sigma.

Western Blot—Whole cell lysates were prepared in radioimmune precipitation buffer (50 mM Tris-HCl (pH 7.4), 150 mM NaCl, 1% Nonidet P-40, 0.25% sodium deoxycholate, 0.1% SDS, 0.5 mM EDTA, 1 mM EGTA, 1 mM dithiothreitol) plus protease inhibitor (from Sigma); 50–100 μg of total protein were resolved by SDS-PAGE, transferred onto polyvinylidene difluoride membranes, blocked in 5% nonfat dry milk/TBST (20 mM Tris-HCl (pH 7.5), 150 mM NaCl, 0.05% Tween 20), and incubated with primary antibodies overnight at 4 °C. Membranes were washed three times for 10 min each in TBST and incubated with horseradish peroxidase-conjugated secondary antibodies for 1–3 h at room temperature. After three 10-min washings, membranes were incubated with enhanced ECL reagent (from Pierce) for 1 min and exposed to x-ray films. To detect Rb protein in MEFs, 5 μg of anti-Rb (851) was mixed with 1 mg of whole cell lysate, and the immune complex was collected on protein A-Sepharose, resolved by SDS-PAGE, and then immunoblotted with anti-Rb antibody from Pharmingen.

Propidium Iodide Uptake—Cells were trypsinized and resuspended in 500 μl of phosphate-buffered saline containing 1 μg/ml propidium iodide, incubated for 10 min at room temperature, and immediately analyzed by flow cytometry, counting at least 10,000 events/sample. For each treatment condition, triplicate samples were analyzed, from which the average percentage of propidium iodide-positive cells was calculated.

DEVDase and IETDase Assay—Cells were lysed in PIPES/CHAPS buffer (10 mM HEPES-KOH (pH 7.5), 10 mM KCl, 1.5 mM $MgCl_2$, 1 mM EDTA, 1 mM EGTA) and clarified by centrifugation. 100 μg of total protein was incubated with 50 μM Ac-DEVD-AMC or Ac-IETD-AFC for 60 min at 37 °C. Fluorometric detection of AMC and AFC was performed in triplicates by excitation at 360 nm/emission at 460 nm (AMC) or excitation at 400 nm/emission at 505 nm (AFC).

Cell Fractionation—Cells were trypsinized, washed in phosphate-buffered saline, resuspended in mannitol/sucrose buffer (210 mM mannitol, 70 mM sucrose, 10 mM HEPES (pH 7.5), 0.5 mM EDTA) plus protease inhibitor and broken up by passage through a 22.5-gauge needle. Heavy membrane fractions (containing mitochondria) were pelleted by centrifugation. 100 μg

---

[3] B. N. Chau and J. Y. J. Wang, unpublished results.
[4] T.-T. Chen and J. Y. J. Wang, unpublished results.

of the supernatant was resolved on a 14% SDS-polyacrylamide gel followed by immunoblotting with anti-cytochrome *c* or anti-Samc.

In Vitro Cytochrome c Release Assay—Freshly isolated liver mitochondria were combined with cytosolic extracts from untreated or TNF-treated *Rb-wt* or *Rb-MI* cells diluted in KCl buffer (125 mM KCl (pH 7.4), 10 mM HEPES-KOH, 5 mM Na_2HPO_4, 4 mM $MgCl_2$, 0.5 mM EGTA) and incubated for 45 min at 37 °C under gentle agitation. Mitochondria were pelleted by centrifugation. The supernatants and the pellets were separately analyzed for cytochrome *c* and Cox-IV by immunoblotting.

In Vivo Affinity Labeling of Caspase-8—We adopted the method described by Tu et al. (41) to label activated caspase-8 in cells. Briefly, 1×10^7 cells were trypsinized, centrifuged, and resuspended in 4 ml of Dulbecco's modified Eagle's medium containing 10% fetal bovine serum with 50 μM biotin-VAD-fmk. After 1 h of incubation at 37 °C, 10 ng/ml hTNF plus CHX (2.5 μg/ml) were added. Cells were harvested at the indicated time and lysed in 0.5 ml of radioimmune precipitation buffer, and 1 mg of total proteins were incubated with 50 μl of streptavidin/Sepharose beads (Amersham Biosciences) at 4 °C overnight. The beads were washed with radioimmune precipitation buffer and boiled in 25 μl of 3× SDS sample buffer, the supernatant was resolved by SDS-PAGE, and caspase-8 was detected by immunoblotting.

Synchronization of Endocytosis—*Rb-wt* or *Rb-MI* cells were first incubated with different doses of hTNF/CHX at 4 °C for 90 min and then shifted to 37 °C for different amounts of time. Cells were subjected to either cell death assay by propidium iodide uptake or DEVDase and IETDase assay.

Dextran Sulfate Sodium (DSS)-induced Colonic Apoptosis in Mice—$Rb^{+/+}$, $Rb^{+/MI}$, or $Rb^{MI/MI}$ mice were fed water containing 3% DSS (M_r 36,000–50,000 from Sigma). At 56 h into DSS feeding, they were injected intraperitoneally with either bafilomycin A1 at a concentration of 25 ng/g body weight or vehicle. Mice were sacrificed 16 h later, and colonic tissues were collected in a roll, fixed in 4% paraformaldehyde for 2 days, embedded into paraffin blocks, cut into 5-μm sections, deparaffined, and TUNEL-labeled. Fluorescent images of labeled sections were captured by CCD camera; TUNEL-positive nuclei were counted in at least 25 crypts per tissue samples. All animal studies were approved by the University of California San Diego institutional animal care and use committee.

Lysosomal pH Measurement—We adopted the method described by Trombetta *et al.* (42) to measure the luminal pH of endosomes and lysosomes. Briefly, 10,000 *Rb-wt* or *Rb-MI* mouse fibroblasts were plated per well in a 96-well plate. After overnight culture, cells were loaded with the pH-sensitive FITC-dextran (Sigma) for 1 h at 37 °C, followed by treatment with hTNF/CHX or bafilomycin A1 (200 nM) for 5 h. At the end of the experiment, excess FITC-dextran was removed by extensive washing with Dulbecco's modified Eagle's medium, and the wells were replaced with phosphate-buffered saline. The fluorescence emitted at 520 nm was recorded at two excitation wavelengths, 450 and 490 nm, using a SpectraMax Gemini fluorescence plate reader. The pH values were determined by comparing the fluorescence signals with a standard curve constructed for FITC-dextran in phosphate/citrate buffers of different pH values between 4.0 and 8.0.

DNA Microarray—*Rb-MI* or *Rb-wt* cells were subjected to different treatments, and then the total RNA was extracted, and the cRNA probes were synthesized and labeled with biotin (for Affymetrix GeneChip® (MGU74A)) or Cy5 or Cy3 (for Agilent mouse whole genome array (G4112A)). Array hybridization, data collection, and analysis were conducted using protocols and programs supplied by the manufacturers and indicated in the figures and tables.

siRNA Experiments—Sense and antisense RNA oligonucleotides corresponding to the target sequence for mouse *Rb* (GUUGAUAAUGCUAUGUCAA), mouse *ATP6V1B1* (TCC-ACCTCAGTCCTATATA), and *LacZ* (AACGTACGCGGAA-TACTTCGA) were synthesized and annealed by Ambion. Uniqueness of individual target sequences was confirmed by a BLAST search of the mouse genomic plus transcript data base. Transfection of synthetic siRNA was performed using Lipofectamine reagent with standard procedures. 48 h after transfection, cells were collected, and target protein levels were analyzed. Cotransfection of Cy3-labeled siRNA duplexes was performed to determine transfection efficiency when necessary.

RESULTS

TNFR1-induced Type-2 Apoptotic Pathway Is Blocked in Rb-MI Cells—We have previously shown that *Rb-MI* mouse fibroblasts are resistant to apoptosis induced by the type-1 TNF receptor (TNFR1), which is activated by human TNF or an anti-TNFR1 agonist antibody (30). Consistent with previous results, hTNF (activates only the mouse TNFR1) or mouse TNF/CHX (mTNF; activates TNFR1 and R2) led to caspase activation measured by the cleavage of DEVD-AMC or IETD-AFC in *Rb-wt* cells (Fig. 1, *A* and *B*). In *Rb-MI* fibroblasts, mTNF/CHX but not hTNF/CHX caused caspase activation (Fig. 1, *A* and *B*). We also measured the IETDase activity, which is mostly mediated by caspase-8 (43), at several concentrations of mTNF and hTNF. With the *Rb-wt* cells, the half-maximum IETDase measured at 5 h after stimulation was observed at a ~10 ng/ml concentration of either hTNF or mTNF, although the maximal levels of IETDase were higher in mTNF/CHX-treated *Rb-wt* cells. With the *Rb-MI* cells, the IETDase activity stimulated by mTNF/CHX was about 2-fold lower than that found in *Rb-wt* cells at every mTNF concentration tested (Fig. 1*C*). With hTNF, however, *Rb-MI* cells appeared nonresponsive, with no detectable stimulation of IETDase at hTNF concentrations up to 80 ng/ml (Fig. 1*C*).

We have previously shown that hTNF/CHX-induced cytochrome *c* release is defective in *Rb-MI* cells (30). As shown in Fig. 1*D*, cytosolic Smac and cytochrome *c* were detected in *Rb-wt* cells treated with hTNF/CHX or mTNF/CHX, but their release only occurred in mTNF/CHX-treated *Rb-MI* cells. Consistent with the role of Bid cleavage in TNF-induced cytochrome *c* release (34, 44), we observed Bid cleavage in *Rb-wt* cells treated with hTNF/CHX or mTNF/CHX, but Bid was only cleaved in mTNF/CHX-treated *Rb-MI* cells (Fig. 1*E*). To further examine the cytochrome *c* release defect in *Rb-MI* cells, we prepared lysates from hTNF/CHX-treated *Rb-wt* and *Rb-MI*

cells and incubated them with liver mitochondria. Cytochrome *c* release activity was detected in lysates from hTNF/CHX-treated *Rb-wt* cells but not those from *Rb-MI* cells (Fig. 1*F*). The lysates of *Rb-MI* cells, either before or after hTNF/CHX treatment, did not interfere with cytochrome *c* release induced by a recombinant NC-Bid (45) (Fig. 1*G*), suggesting that the defect is not caused by an inhibitor of tBid in *Rb-MI* lysates. In keeping

with this conclusion, we found that hTNF/CHX induced similar modifications of Mcl-1, an inhibitor of cytochrome *c* release, in *Rb-wt* and *Rb-MI* cells (supplemental Fig. 1*B*). We also prepared liver mitochondria from *Rb-MI* mice and found them to be competent in releasing cytochrome *c* in response to lysates from hTNF/CHX-treated *Rb-wt* fibroblasts (Fig. 1*H*). Taken together, these results show that TNFR1-induced Bid cleavage
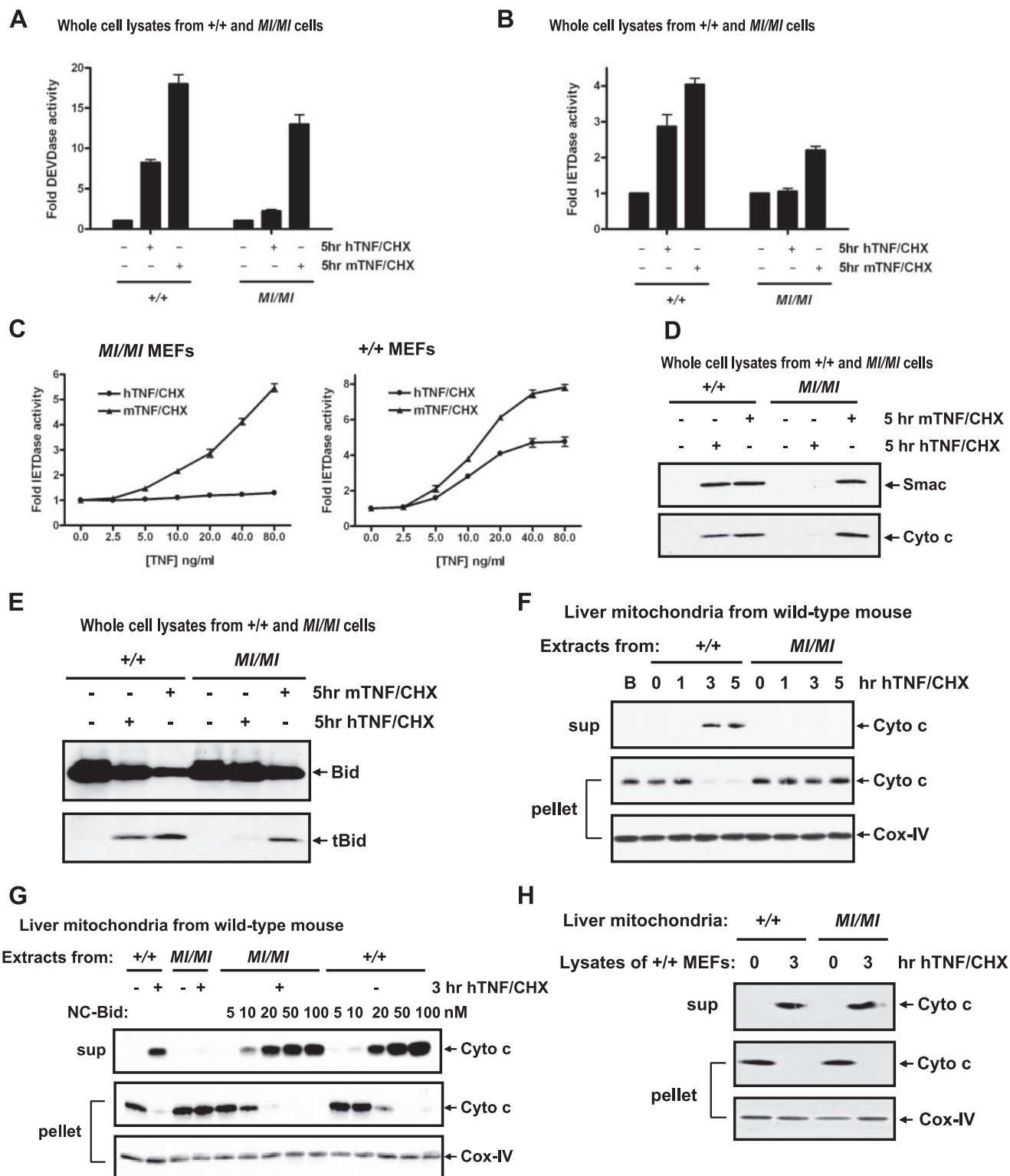
is defective in *Rb-MI* cells and that the lack of tBid rather than the accumulation of inhibitors accounted for the cytochrome *c* release defect in hTNF/CHX-treated *Rb-MI* cells.

TNFR1-induced Cleavage of Rb Requires Caspase-8—TNF-induced Bid cleavage is dependent on caspase-8 (34, 44). Likewise, TNFR1-induced Rb cleavage is also dependent on caspase-8 (Fig. 2, *A–D*). Treatment with hTNF/CHX did not cause the cleavage of Rb, PARP1, or caspase-3 in fibroblasts derived from caspase-8 knock-out mouse (Fig. 2*B*); nor did it activate the DEVDase or IETDase activity (Fig. 2, *C* and *D*). Cleavage of Rb, PARP1, and caspase-3 and activation of DEVDase or IETDase in response to hTNF/CHX occurred in fibroblasts from *Caspase-8*$^{+/+}$ littermates (Fig. 2, *B–D*). Since caspase-8 is required for TNFR1 to induce the cleavage of Rb and Bid, and since Bid cleavage is defective in *Rb-MI* cells, our results (Figs. 1 and 2) suggest that Rb cleavage is required for Bid cleavage.

TNFR1-induced Bid Cleavage Is Restored by the Knockdown of Rb-MI—To demonstrate that the Rb-MI protein is required to prevent Bid cleavage, we used siRNA to knockdown its expression (Fig. 2*E*). The knockdown of wild type Rb protein did not enhance hTNF/CHX-induced IETDase activity, Bid cleavage, or cell death (Fig. 2, *F–H*). In contrast, knockdown of Rb-MI restored hTNF/CHX-induced IETDase activity, Bid cleavage, and cell death (Fig. 2, *F–H*). These results suggest that Rb cleavage is sufficient to promote TNFR1-induced Bid cleavage, because the knockdown of Rb does not further enhance Bid cleavage. By contrast, the Rb-MI protein, which cannot be cleaved, blocks Bid cleavage. Furthermore, the Rb-MI protein must be present to prevent TNFR1 from inducing the cleavage of Bid, because Bid cleavage is restored with the knockdown of Rb-MI.

TNF-induced Gene Expression Is Similar in Rb-wt and Rb-MI Cells—Given the established role of Rb in the regulation of gene expression, we performed microarray analyses to compare gene expression profiles of *Rb-MI* cells treated with hTNF/CHX *versus* mTNF/CHX. However, we did not detect any statistically significant differences despite the fact that mTNF/CHX, but not hTNF/CHX, induced Bid cleavage in *Rb-MI* cells (supplemental Fig. 2 and Table 1). We also compared hTNF/CHX-induced gene expression changes in *Rb-wt* and *Rb-MI* cells and found a similar cohort of up-regulated and down-regulated genes in these two cell lines (supplemental Table 2). We have previously observed hTNF/CHX-induced IκB-α degradation in *Rb-wt* and *Rb-MI* cells (30), consistent with the similar up-regulation of several known NF-κB regulated genes by TNF in these cells (supplemental Table 2). We also found that hTNF/CHX-induced phosphorylation of c-Jun was similar in *Rb-wt* and *Rb-MI* cells (supplemental Fig. 1*A*). Thus, Rb-MI did not exert a detectable effect on TNF-induced gene expression, which is mediated by the TNFR1 at the plasma membrane. Moreover, a Bid cleavage defect in *Rb-MI* cells is not likely to require new gene expression, since it is observed in the presence of CHX.

Activation of Caspase-8 in Rb-MI Cells—We have previously observed the loss of full-length caspase-8, occurring between 12 and 24 h after hTNF/CHX treatment in both *Rb-wt* and *Rb-MI* primary fibroblasts (30), indicating that caspase-8 activation is not impaired in *Rb-MI* cells. With the immortalized *Rb-wt* and *Rb-MI* fibroblasts, we could not detect any reduction in full-length caspase-8 at 5 h after hTNF/CHX treatment when Bid cleavage was observed (Fig. 3*A*). Since caspase-8 activation does not require its cleavage (46, 47), we adopted an *in vivo* affinity labeling method to covalently biotinylate activated caspase-8 with a membrane-permeable biotin-VAD-fmk (41) (Fig. 3*B*). The full-length (p55) caspase-8 was pulled down by streptavidin beads only in cells exposed to biotin-VAD-fmk (not shown), and this p55 band was not found in *caspase-8*$^{-/-}$ fibroblasts (Fig. 3*C*). The levels of biotinylated p55 caspase-8 were similar in untreated and hTNF/CHX-treated cells (Fig. 3, *C* and *D*). Detection of active caspase-8 in untreated cells may not be surprising, given the recent finding that caspase-8 has biological functions other than the stimulation of apoptosis (48, 49). At 2 h after hTNF/CHX addition, a p43 caspase-8 band was pulled down in cells with caspase-8 but not in the *Caspase-8*$^{-/-}$ cells (Fig. 3, *C* and *D*). Previous studies have shown that the p43 caspase-8 is present in the endosomal fraction of TNF-treated cells (16). Approximately 1% of the input p55 band was pulled down by the streptavidin beads (Fig. 3*D*), and the p43 band could not be detected in whole cell lysates (Fig. 3*A*), indicating that only a small fraction of the full-length caspase-8 was activated and converted to p43 in response to hTNF/CHX. We observed biotinylated p55 and p43 bands in hTNF/CHX-treated *Rb-wt* and *Rb-MI* cells (Fig. 3*D*), consistent with the previous conclusion that TNFR1-induced caspase-8 activation does occur in *Rb-MI* cells.

FIGURE 1. **TNFR1-induced type-2 apoptotic pathway is blocked in *Rb-MI* MEFs.** *A* and *B*, DEVDase (*A*) and IETDase (*B*) activities were not activated by hTNF/CHX in *Rb-MI* MEFs. The protease activities in whole cell lysates were measured at 5 h after the indicated treatments. Activity in untreated lysate was set to 1 for each cell type. Values are mean and S.E. from three independent experiments. *C*, IETDase dose response to hTNF/CHX or mTNF/CHX. *Rb-MI* or *Rb-wt* cells were treated with the indicated concentrations of hTNF or mTNF plus CHX (2.5 μg/ml). The IETDase activity in whole cell lysates was measured at 5 h after the indicated treatments, and the activity in untreated lysates was set to 1. Values are mean and S.E. from three independent experiments. *D*, cytosolic cytochrome *c* (*Cyto c*) and Smac were not detected in hTNF/CHX-treated *Rb-MI* cells. *Rb-wt* (+/+) and *Rb-MI* (*MI/MI*) cell lysates were prepared 5 h after the indicated treatments. Equal amounts of cytosolic protein were resolved by SDS-PAGE and immunoblotted with anti-cytochrome *c* or anti-Smac. *E*, Bid is not cleaved in hTNF/CHX-treated *Rb-MI* cells. Whole cell lysates were prepared at 5 h after the indicated treatment. Equal amounts of total protein were resolved by SDS-PAGE, and Bid and tBid were detected by immunoblotting. *F*, cytosolic extracts from hTNF/CHX-treated *Rb-wt* but not *Rb-MI* cells induced cytochrome *c* release from liver mitochondria. Cytosolic extracts from cells prepared at the indicated time after hTNF/CHX treatment were incubated with mouse liver mitochondria at 37 °C for 45 min. Mitochondria were pelleted by centrifugation, and supernatants and pellets were analyzed for cytochrome *c* and Cox-IV by immunoblotting. *B*, buffer-treated mitochondria. *G*, cytosolic extracts from *Rb-MI* cells did not interfere with cytochrome *c* release stimulated by recombinant truncated Bid (*NC-Bid*) (46). The indicated extracts from hTNF/CHX-treated (+) or untreated (−) cells were incubated with liver mitochondria from wild type mice plus the indicated amounts of NC-Bid, and the incubation mixtures were analyzed for cytochrome *c* release as in *E*. *H*, liver mitochondria from *Rb*$^{MI/MI}$ mice released cytochrome *c* in response to cytosolic extract from hTNF/CHX-treated *Rb-wt* cells. Cytosolic extracts were prepared after the indicated treatment and incubated with mitochondria isolated from the liver of *Rb*$^{+/+}$ or *Rb*$^{MI/MI}$ mice. Cytochrome *c* release was examined as in *F*.
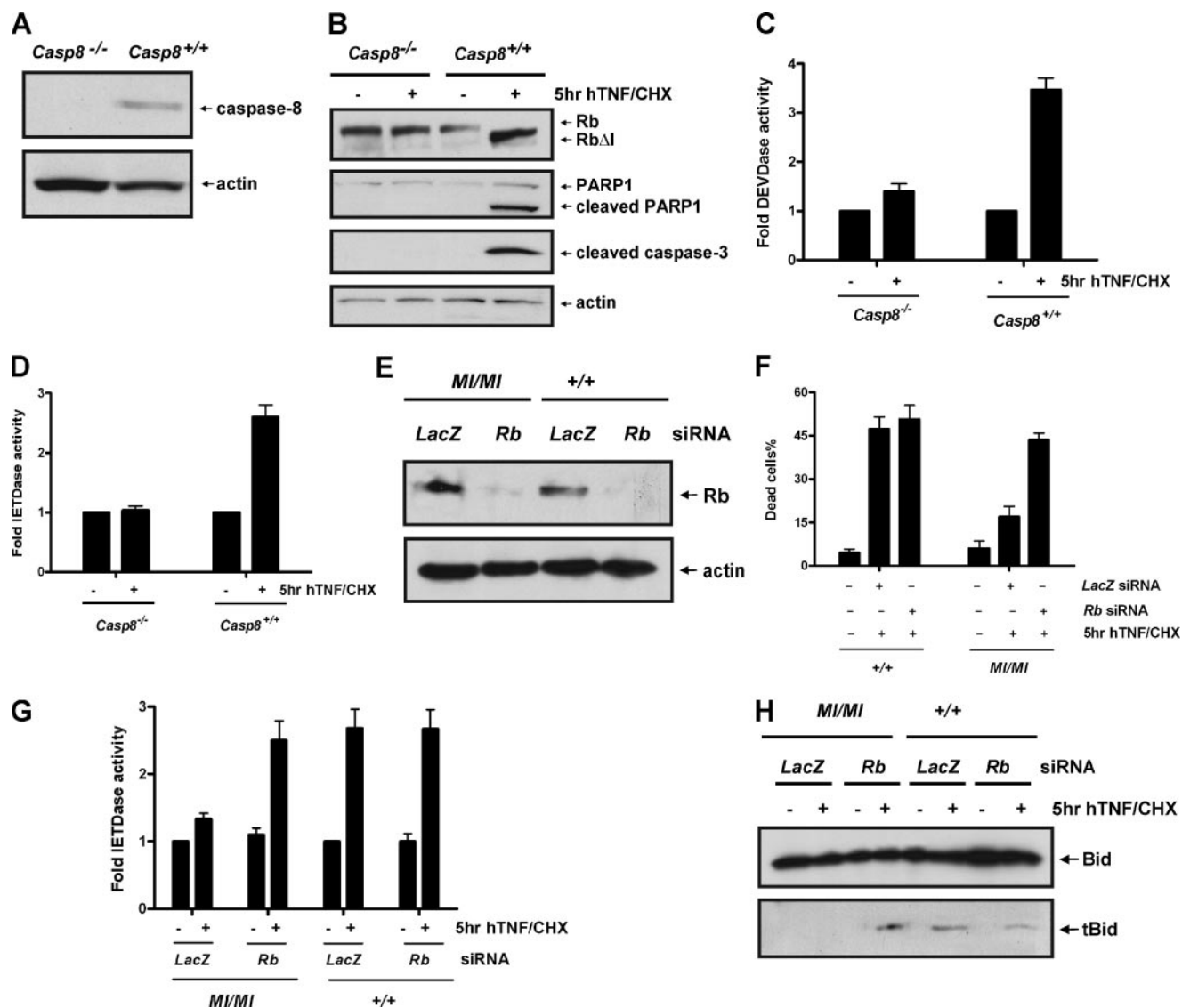
FIGURE 2. **TNF-induced Rb cleavage is dependent on caspase-8 and required for Bid cleavage.** *A*, caspase-8 (p55) is detected in wild-type (*Casp8*$^{+/+}$) but not caspase-8 knock-out (*Casp8*$^{-/-}$) cells. *B*, cells with the indicated genotypes were treated with hTNF/CHX for 5 h and analyzed for PARP1 and cleaved caspase-3 by immunoblotting of whole cell lysates. The cleavage of Rb was detected by immunoprecipitation (*IP*) and immunoblotting (*IB*) as described under "Experimental Procedures." The levels of actin are shown as loading controls. *C* and *D*, DEVDase (*C*) or IETDase (*D*) activity was measured in whole cell lysates after a 5-h treatment of the indicated cells with hTNF/CHX, with the activity in untreated lysates set to 1. Values are mean and S.E. from three independent experiments. *E*, the indicated cells were transfected with control siRNA (*LacZ*) or Rb siRNA, and the level of Rb protein was determined by IP/IB at 48 h post-transfection. *F*, Rb siRNA restored death response to hTNF/CHX in *Rb-MI* MEFs. At 48 h post-transfection, cells of the indicated genotypes were treated with hTNF/CHX for 5 h, and cell death was determined by the uptake of propidium iodide. Values are mean and S.E. from three independent experiments. *G*, Rb siRNA enhanced hTNF/CHX-induced IETDase activity in *Rb-MI* cells. Cells treated as in *F* were collected, and the IETDase activity was measured in whole cell lysates. -Fold changes are relative to LacZ siRNA-transfected and untreated cells for each genotype. Means and S.E. from three independent experiments are shown. *H*, Rb siRNA allowed Bid cleavage in hTNF/CHX-treated *Rb-MI* MEFs. Whole cell lysates from *G* were analyzed for Bid and tBid by immunoblotting.

Enhanced Death Response, Caspase Activity, and Bid Cleavage through 4 °C Preincubation with TNF—Recent reports have suggested that TNFR1 endocytosis is required for the activation of caspase-8 (16, 17), and synchronized endocytosis enhances TNFR1-induced caspase-8 activation (16). Synchronized endocytosis can be achieved by preincubating cells with TNF at 4 °C and then raising the temperature to 37 °C to allow for the simultaneous uptake of ligand-engaged TNFR1 (16). We applied this protocol to the *Rb-wt* and *Rb-MI* cells at varying concentrations of hTNF and found that synchronization sensitized both cell types to hTNF/CHX-induced death, measured at 24 h post-temperature shift (Fig. 4, *A* and *B*). The preincubation protocol

also enhanced IETDase activity measured at 2–3 h after the hTNF/CHX addition (Fig. 4*C*), corresponding to the cleavage of Bid (and the formation of tBid) in *Rb-MI* cells (Fig. 4*D*). Although preincubation enhanced the response of *Rb-MI* cells to hTNF/CHX, it did not restore the response to that of the *Rb-wt* cells. Nevertheless, the partial rescue of Bid cleavage defect by preincubation suggests that the level of caspase-8 can be artificially raised in *Rb-MI* cells by synchronized endocytosis. The endocytosis of TNF receptor should be functional in *Rb-MI* cells; otherwise, we would not have been able to sensitize these cells by preincubation at 4 °C. However, the apoptotic signal output from the endocytic compartment is lower in
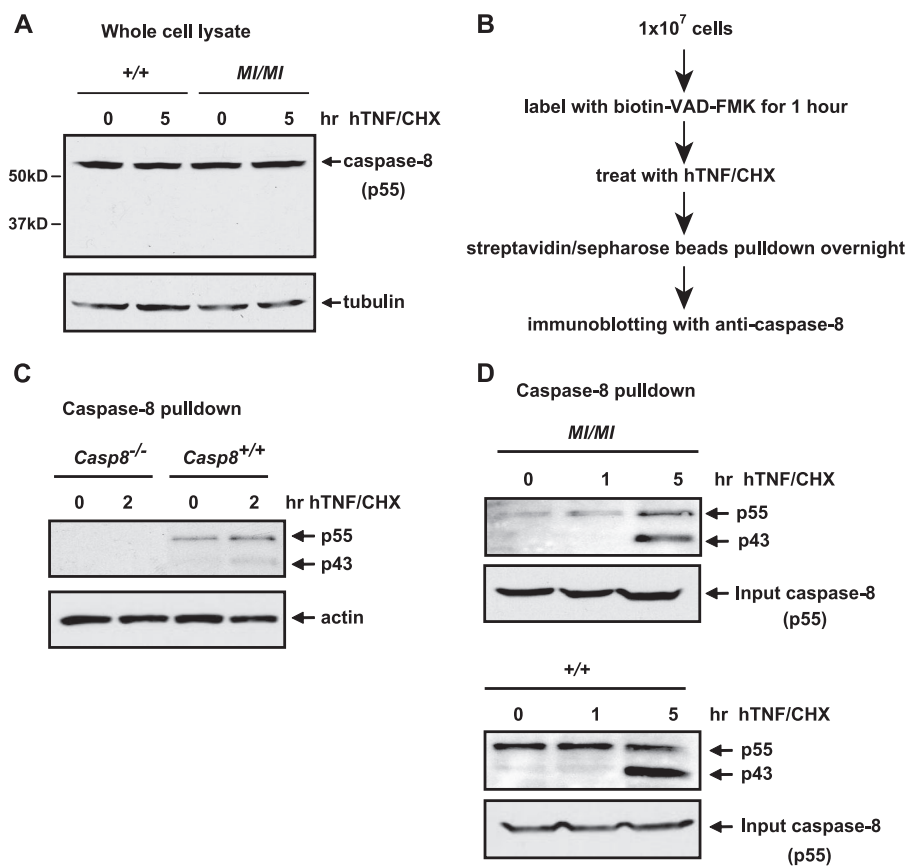
A

Whole cell lysate

B

C

Caspase-8 pulldown

D

Caspase-8 pulldown

FIGURE 3. *In vivo* **affinity labeling of activated caspase-8 in *Rb-wt* and *Rb-MI* cells.** *A*, caspase-8 processing was not detected in whole cell lysates prepared at 5 h after hTNF/CHX treatment of *Rb-wt* or *Rb-MI* MEFs. *B*, outline of the affinity labeling experiments. *C*, biotinylation of caspase-8. Cells of the indicated genotypes were treated as in *B*. The p55 and p43 bands were not present in caspase-8 knock-out MEFs. The levels of actin in the input fractions are shown. *D*, biotinylation of caspase-8 in *Rb-wt* and *Rb-MI* cells. Cells of the indicated genotypes were collected at the indicated time after hTNF/CHX treatment, whole cell lysates (1 mg of total protein) were incubated with streptavidin beads, and caspase-8 was detected in the bound fractions by immunoblotting. The amounts of p55 caspase-8 in 50 μg of each input fraction are also shown.

Rb-MI cells than that of *Rb-wt* cells even under conditions of synchronized endocytosis.

One possibility for the Bid cleavage defect might be that activated caspase-8 was lost through endosomal trafficking in *Rb-MI* cells. We tested several drugs known to interfere with endocytic trafficking and lysosomal degradation for their effects on hTNF/CHX-induced IETDase activity in *Rb-MI* cells (Fig. 4*E*). Four of the compounds tested (*i.e.* ammonium chloride (raises intracellular pH), FCCP (a proton ionophore), 3-methyladenine (3-MA) (an inhibitor of autophagy), and benzyloxycarbonyl-FF-fmk (an inhibitor of cathepsins)) did not activate IETDase in the absence or presence of hTNF/CHX (Fig. 4*E*). Interestingly, we found that concanamycin A and bafilomycin A both are inhibitors of V-ATPase and stimulated IETDase activity in hTNF/CHX-treated *Rb-MI* cells but did not have any effect in the absence of TNF (Fig. 4*E*). V-ATPase acidifies the endosomes to promote their trafficking along the lysosomal degradative pathway (39). We therefore measured the pH of the endosomal compartment using a pH-sensitive fluorescent dextran (50) and found that hTNF/CHX treatment did not affect the endosomal pH in *Rb-wt* or *Rb-MI* cells (Fig. 4*F*). By contrast, treatment with bafilomycin A1 (*Baf*) raised the endosomal pH from 5.5 to 7 irrespective of TNF treatment in

both *Rb-wt* and *Rb-MI* cells (Fig. 4*F*). Thus, TNF does not cause a detectable inhibition of V-ATPase activity; however, V-ATPase inhibitor can restore TNF-induced IETDase in *Rb-MI* cells.

Inhibition of V-ATPase Restores Caspase-8-dependent Bid Cleavage in Rb-MI Cells—To further examine the effect of V-ATPase inhibition, we tested whether Baf can enhance the activation of caspase-8. Using the *in vivo* biotinylation approach outlined in Fig. 3*B*, we showed that Baf did not cause a significant increase in the pull-down of p55 and p43 caspase-8 in *Rb-wt* and *Rb-MI* cells (Fig. 5*A*). However, Baf allowed the accumulation of cytosolic IETDase activity and the cleavage of Bid in hTNF/CHX-treated *Rb-MI* cells (Fig. 5, *B* and *C*). Baf treatment did not enhance IETDase activity or Bid cleavage in *Rb-wt* cells. Bid cleavage under the condition of Baf plus hTNF/CHX remained dependent on caspase-8 (Fig. 5*D*), showing that Baf did not activate an alternative Bid cleavage pathway. We found that the levels of TNFR1 and DISC component proteins were similar in *Rb-wt* and *Rb-MI* cells, and their levels were not affected by hTNF/CHX and/or Baf treatment (Fig. 5*E*). We noted that Baf also stimulated hTNF/CHX-induced Rip1 cleavage, which is mediated by caspase-8 (51), in *Rb-MI* cells but not in *Rb-wt* cells (Fig. 5*E*).

To seek additional evidence that inhibition of V-ATPase can restore Bid cleavage in *Rb-MI* cells, we knocked down the B1 subunit of the cytosolic V$_1$ complex of the V-ATPase by siRNA. The control siRNA did not affect Bid cleavage; however, the knockdown of the V-ATPase B1 subunit rescued hTNF/CHX-induced IETDase activity and Bid cleavage in *Rb-MI* cells (Fig. 5, *F–H*). Because pretreatment with Baf or V1B1 knockdown did not enhance hTNF/CHX-induced IETDase or Bid cleavage in *Rb-wt* cells (Fig. 5, *B*, *C*, *E*, *F*, and *G*), it suggests that V-ATPase inhibition is irrelevant to Bid cleavage when Rb can be cleaved. However, in *Rb-MI* cells, V-ATPase inhibition supplants the requirement of Rb cleavage to allow Bid cleavage.

Bafilomycin A1 Stimulates DSS-induced Colonic Apoptosis in Rb$^{MI/MI}$ Mice—We have previously shown that *Rb-MI* promotes colon tumors in the *p53-null* genetic background, correlating with reduced apoptotic response to inflammation-associated epithelial apoptosis (52). We induced apoptosis of colonic epithelial cells by feeding mice with water containing DSS for 3 days (52). Mice were also exposed to Baf via intraperitoneal injection 16 h prior to the collection of colonic tissue. Exposure to DSS induced TUNEL-positive nuclei in the colonic

epithelium (Fig. 6*A*). Exposure to Baf alone did not induce apoptosis (not shown). Following DSS exposure, the number of TUNEL-positive nuclei in the colonic crypts was significantly lower in $Rb^{MI/MI}$ mice than in $Rb^{+/+}$ littermates (Fig. 6*B*). However, additional exposure to Baf significantly increased the apoptotic response of $Rb^{MI/MI}$ mice to DSS feeding. Baf also signifi-

A

B

C

D

E

F
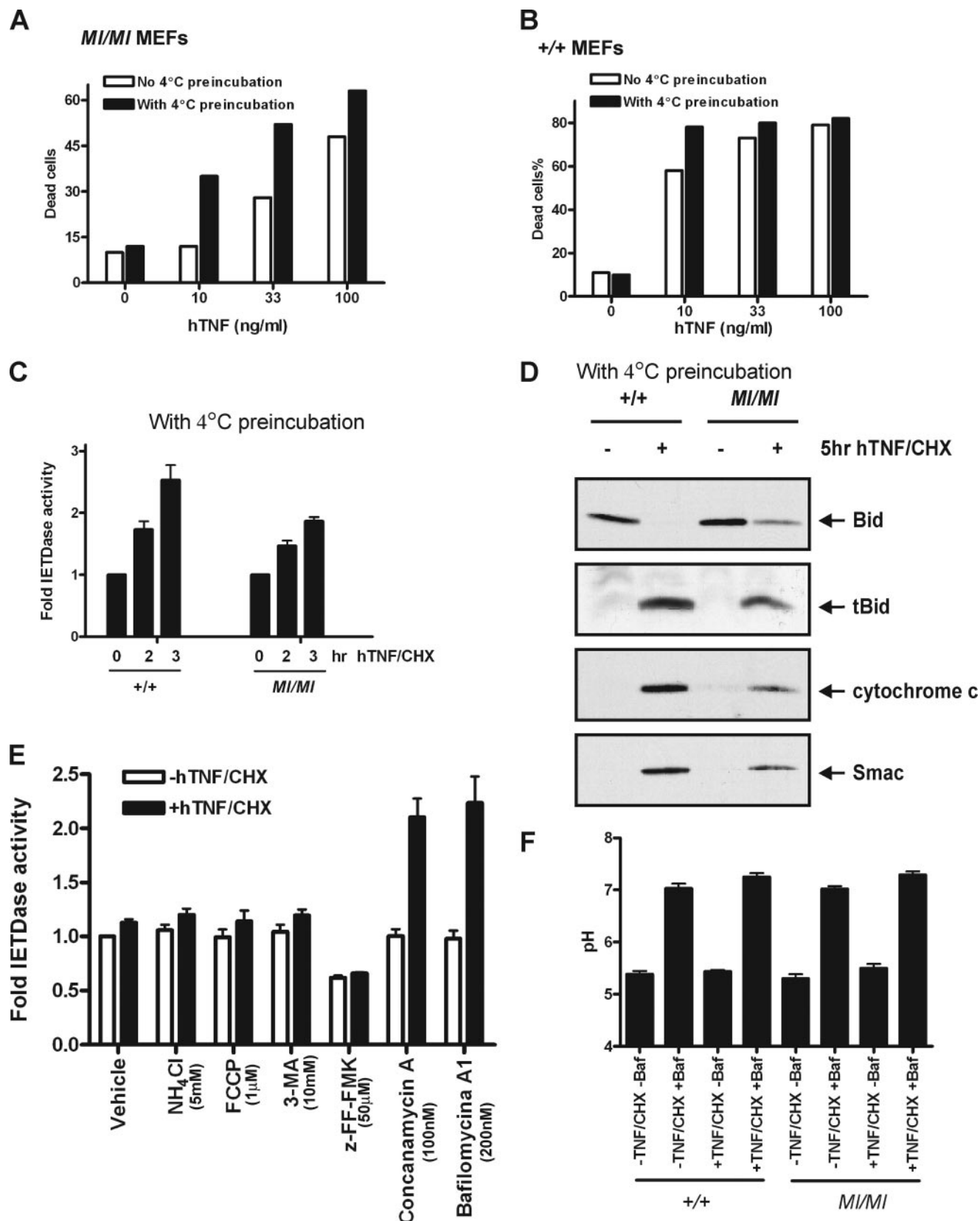
cantly enhanced the apoptotic response of $Rb^{+/MI}$ mice to DSS (Fig. 6*B*). By contrast, Baf did not affect the colonic apoptotic response in $Rb^{+/+}$ mice (Fig. 6*B*). We have previously shown that thymocytes from $Rb^{MI/MI}$ mice are resistant to hTNF/CHX-induced apoptosis (31). We found that treatment with Baf also enhanced hTNF/CHX-induced apoptosis of thymocytes from $Rb^{MI/MI}$ but not $Rb^{+/+}$ mice (not shown). Thus, *Rb-MI*-mediated inhibition of TNFR1-dependent apoptosis can be overridden by Baf in fibroblasts, thymocytes, and colonic epithelial cells.

DISCUSSION

Sequential Activation of TNFR1-induced Type-1 and Type-2 Apoptotic Pathways—In the current model of extrinsic apoptotic pathways, activation of caspase-8 leads to the simultaneous cleavage of substrates in the type-1 and the type-2 pathways (Fig. 7*A*). This parallel cleavage model cannot explain our observations with the *Rb-MI* cells, where caspase-8 is activated but Bid is not cleaved. Our results suggest an alternative model where caspase-8-dependent Rb cleavage precedes caspase-8-dependent Bid cleavage (Fig. 7*B*). Because Bid is not cleaved in *Rb-MI* cells, we propose that Rb cleavage via the type-1 pathway is an upstream requirement for Bid cleavage in the type-2 pathway (Fig. 7*B*).

The sequential cleavage model predicts that Rb cleavage would not be required for TNF to kill cells that die by the type-1 pathway alone. In other words, Rb-MI would only protect type-2 cells from TNF-induced apoptosis. This is consistent with our previous findings that endotoxin-induced apoptosis is blocked in the intestine but not in the spleen of *Rb-MI* mice (30). We would point out that mouse embryo fibroblasts (MEFs) are type-1 cells, because TNF/CHX-induced apoptosis is observed in *Bid* knock-out and *cytochrome c* knock-out MEFs (53, 54). In other words, the Bid-dependent cytochrome *c* release is not necessary for TNF/CHX to kill MEFs. In fact, we show that mTNF/CHX can indeed activate apoptosis in *Rb-MI* MEFs. Only by activating TNFR1 alone with human TNF could we reveal the type-2 pathway blockade imposed by Rb-MI in MEFs. The physiological relevance of the MEF-based experimental results is demonstrated by our observation that bafilomycin A1 can restore colonic apoptosis in DSS-treated $Rb^{MI/MI}$ mice. We have found that DSS-induced colonic apoptosis is diminished in TNFR1-deficient mice,[5] suggesting the involvement of TNFR1 in this *in vivo* response. This death

response is diminished in $Rb^{+/MI}$ and $Rb^{MI/MI}$ mice but could be enhanced by bafilomycin. Taken together, results from *Rb-MI* MEFs and $Rb^{MI/MI}$ mice are consistent with the model that Rb cleavage is required for TNF to activate the type-2 apoptotic pathway.

Receptor Endocytosis and Cytosolic Accumulation of Activated Caspase-8—Previous studies have shown that TNFR1 does not initiate DISC assembly at the plasma membrane (18, 19). Instead, the TNFR1-DISC complex is detected in the endosomal fraction under conditions of synchronized endocytosis in several cell types (16, 17). A cytosolic DISC free of TNFR1 has been observed in a human fibrosarcoma cell line that ectopically expresses a constitutive inhibitor of NF-κB (18). In the fibrosarcoma cell line, two distinct signaling complexes were identified. Complex-1 contains TNFR1, TRADD, RIP1, and TRAF2 and mediates NF-κB activation. This membrane complex appears to be further processed to recruit FADD through TRADD, resulting in the formation of complex-2 (*i.e.* the DISC complex), which dissociates from TNFR1 and accumulates in the cytosol (18). Interestingly, although TRAIL-induced apoptosis does not require receptor endocytosis (55), internalization of FAS/CD95 and TNFR1 through endocytosis is required for the induction of apoptosis (16, 17, 56). Activated FAS/CD95L directly recruits FADD and stimulates a small amount of DISC formation at the cell surface, followed by endocytosis of the entire complex. In type-1 cells, this internalization step triggers further recruitment of FADD and caspase-8 to stimulate apoptosis (56). We have found that *Rb-MI* does not interfere with apoptosis induced by anti-FAS or TRAIL (30).[6] *Rb-MI* does not interfere with TNFR1 endocytosis, because synchronization of endocytosis rescued Bid cleavage in *Rb-MI* cells. Taken together, these results suggest that *Rb-MI* does not block apoptosis at the step of receptor internalization. Furthermore, these results suggest that DISC complexes stimulated by activated Fas *versus* TNFR1 may be subjected to different regulation, despite the similar requirement for receptor endocytosis in the assembly of DISC. Because synchronized endocytosis can enhance caspase-8 activity and Bid cleavage in MEFs, irrespective of Rb cleavage, and because the inhibition of V-ATPase specifically enhanced caspase-8-dependent Bid cleavage in *Rb-MI* cells, Rb-MI is likely to exert its antiapoptotic effect by preventing the cyto-

[5] I. C. Hunton and J. Y. J. Wang, unpublished results.

[6] X. Huang, A. Masselli, S. M. Frisch, I. C. Hunton, Y. Jiang, and J. Y. J. Wang, unpublished results.

FIGURE 4. **Preincubation at 4 °C sensitized *Rb-wt* and *Rb-MI* cells to hTNF/CHX.** *A* and *B*, death response was enhanced by preincubation with hTNF/CHX at 4 °C. Cell death was measured by propidium iodide uptake at 24 h after treatment with the indicated concentrations of hTNF and CHX (2.5 μg/ml) in *Rb-MI* (*A*) and *Rb-wt* (*B*) cells. Cells were treated with or without a 90-min preincubation at 4 °C followed by warming to 37 °C to induce synchronized endocytosis. Note that preincubation sensitized *Rb-wt* and *Rb-MI* cells to hTNF/CHX-induced death. However, death response was lower in *Rb-MI* cells at every hTNF concentration tested. *C*, IETDase activity was enhanced by preincubation with hTNF/CHX at 4 °C. *Rb-wt* and *Rb-MI* cells were incubated with hTNF (33 ng/ml) plus CHX (2.5 μg/ml) at 4 °C for 90 min and then shifted to 37 °C for the indicated times, and the -fold increase in IETDase activity over untreated cells was determined. *D*, Bid cleavage was partially restored in *Rb-MI* cells by preincubation. Cells treated as in *C* were collected at 5 h after warming to 37 °C. Whole cell lysates were analyzed for Bid; cytosolic extracts were analyzed for cytochrome *c* and Smac. *E*, effects of inhibitors on IETDase activity in *Rb-MI* cells. Cells were pretreated with the indicated chemicals for 1 h and then treated with hTNF/CHX for 5 h. IETDase activity was measured in whole cell lysates, and the activity in untreated cell lysate was set to 1. *F*, analysis of lysosomal pH. *Rb-wt* and *Rb-MI* cells were labeled with the pH-sensitive FITC-dextran for 1 h and then were treated with hTNF/CHX, with or without 200 nM bafilomycin A1 as described under "Experimental Procedures." The pH values were determined by comparing the fluorescence intensity with a standard curve constructed for FITC-dextran in phosphate/citrate buffers of different pH values between 4.0 and 8.0.
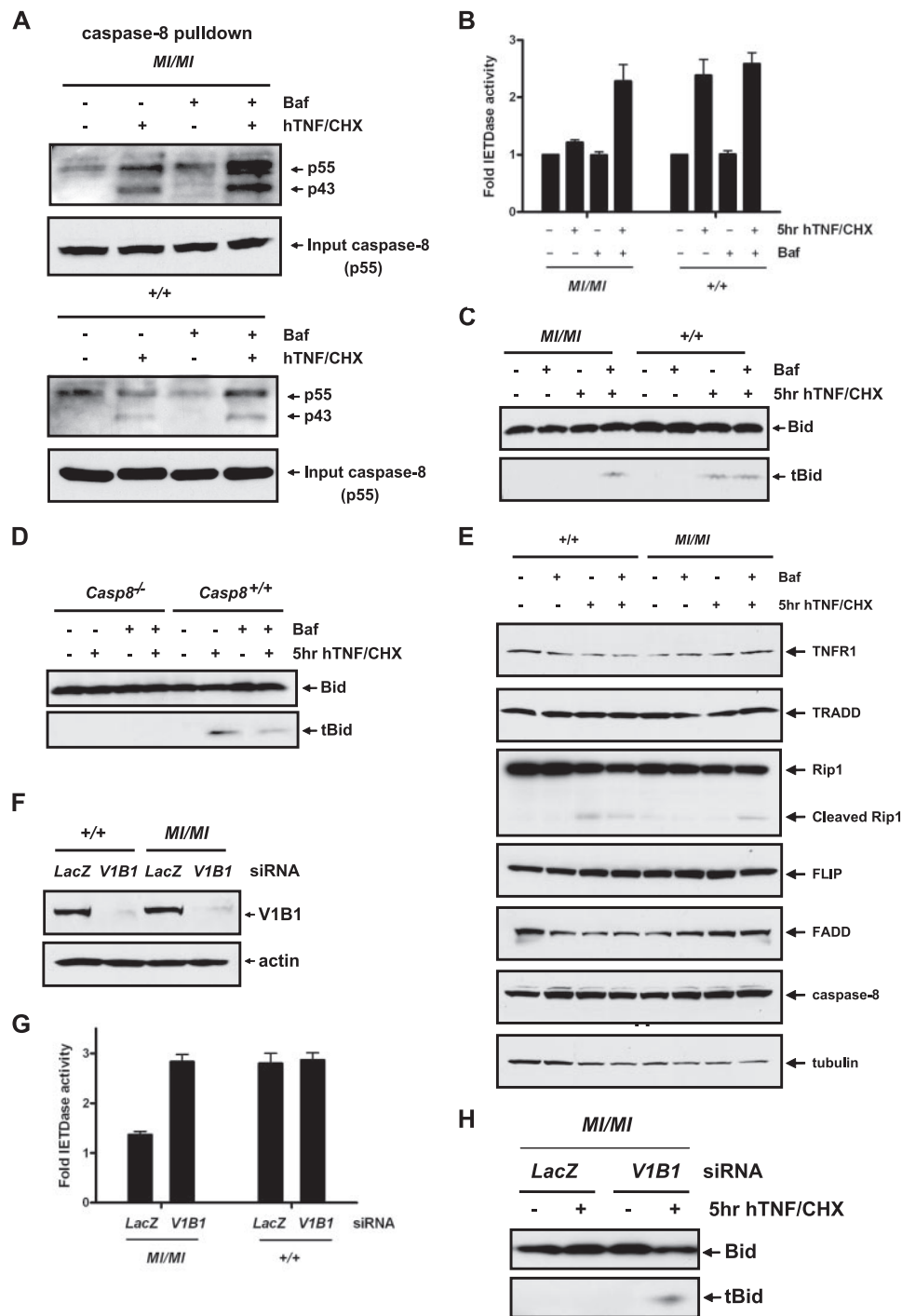
FIGURE 5. **Inhibition of V-ATPase restores Bid cleavage in hTNF/CHX-treated *Rb-MI* MEFs.** *A*, Baf does not significantly affect the biotinylation of caspase-8. Cells of the indicated genotypes were preincubated with 50 μM biotin-VAD-fmk in the absence ($-$) or presence ($+$) of 200 nM Baf for 1 h and then treated with hTNF/CHX for 5 h. Caspase-8 in the input lysates and in the streptavidin pull-down fractions was measured by immunoblotting. *B*, Baf-stimulated IETDase activity in hTNF-treated *Rb-MI* cells. Cells of the indicated genotypes were preincubated with 200 nM Baf for 1 h followed by hTNF/CHX for 5 h, and IETDase activity was measured. The activity of untreated cells of each genotype was set to 1. -Fold changes represent means and S.E. values from three experiments. *C*, Baf rescued hTNF/CHX-induced Bid cleavage in *Rb-MI* cells. Cells treated as in *B* were analyzed for Bid and tBid by immunoblotting of whole cell lysates. *D*, Baf does not induce Bid cleavage in caspase-8 knock-out cells. Cells of the indicated genotypes were treated as in *B*, and whole cell lysates were analyzed for Bid and tBid by immunoblotting. *E*, effects of hTNF/CHX and/or Baf on the levels of TNFR1 and DISC components. *Rb-wt* and *Rb-MI* cells were treated with or without hTNF/CHX for 5 h, in the presence or absence of a 1-h preincubation with bafilomycin A1 (200 nM). Whole cell lysates were immunoblotted with the indicated antibodies. Note that Baf allowed Rip1 cleavage in hTNF/CHX-treated *Rb-MI* cells. *F*, knockdown of the B1 subunit in the V1 complex of the mouse V-ATPase (V1B1). Whole cell lysates collected at 48 h post-transfection with the indicated siRNA were immunoblotted with anti-V1B1 or anti-actin. *G* and *H*, knockdown of V1B1 enhanced IETDase activity (*G*) and Bid cleavage (*H*) in *Rb-MI* cells. At 48 h post-transfection with the indicated siRNA, *Rb-MI* cells were treated with hTNF/CHX for 5 h. Whole cell lysates were analyzed for IETDase activity, with the activity in mock-transfected and untreated sample from each genotype set to 1 (*G*).
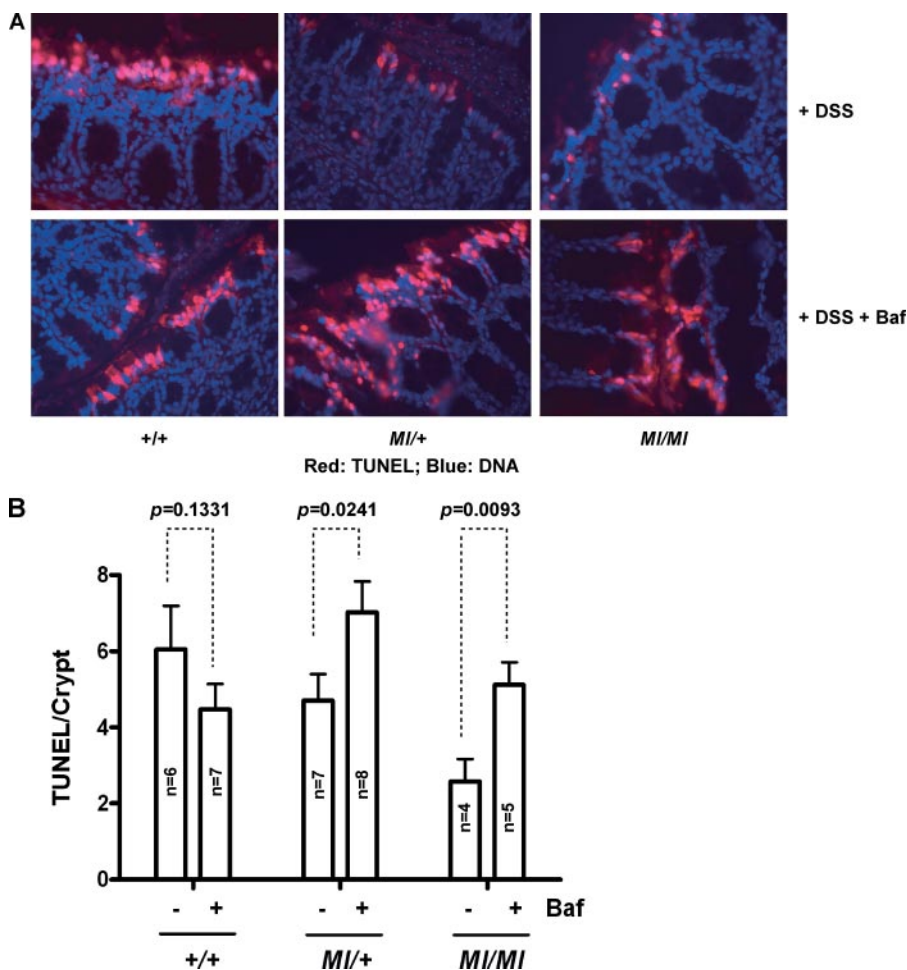
FIGURE 6. DSS-induced colonic epithelial apoptosis is reduced in *Rb^{MI/MI}* mice but restored by bafilomycin A1. *A*, representative images of colonic tissue sections stained with DAPI (*blue*) or TUNEL (*red*). Mice of the indicated genotypes were fed with water containing 3% DSS. At 56 h into DSS feeding, they were injected intraperitoneally with either Baf (25 ng/g body weight) or vehicle (phosphate-buffered saline). Mice were sacrificed 16 h after injection, and colonic apoptosis was quantitated as described under "Experimental Procedures." *B*, density of TUNEL-positive nuclei. The number of TUNEL-positive nuclei per crypt was determined by counting at least 25 full crypts or 50 half crypts in 3–5 sections/sample. The number of mice in each experimental group is shown, and the *p* values were determined by *t* test assuming unequal variances.

Furthermore, hTNF/CHX treatment did not alter the endosomal pH in *Rb-MI* cells. Taken together, these results suggest that Rb cleavage, mediated by the type-1 pathway, may regulate the release/sorting of endosomal DISC, but not the lysosomal degradation of activated caspase-8, to promote Bid cleavage.

Mechanism of Rb-dependent Blockade of Bid Cleavage—The nuclear Rb protein inhibits cell proliferation and apoptosis through transcriptional regulation of E2F-dependent gene expression (58). Cleavage of Rb at the C-terminal caspase site (DEAD^{886}G^{887}) mutated in Rb-MI (DEAA^{886}E^{887}) generates a large Rb-ΔI fragment (residues 1– 886) that encompasses the two well-defined E2F-binding pockets and the Abl-binding C-pocket in the Rb protein (59, 60). We have previously shown that Rb-ΔI is further degraded in apoptotic cells (28, 30), suggesting that C-terminal cleavage can cause the loss of Rb protein thus leading to the activation of proapoptotic gene expression through E2F and Abl (31, 58). The blockade of Bid cleavage observed in this study is not likely to involve new gene expression, because Rb-ΔI was not further degraded at the time point when Bid cleavage occurred and because cycloheximide was used in conjunction with TNF to induce cell death.

solic accumulation of activated caspase-8 downstream of TNFR1 activation.

We propose that the endosomal TNFR1·DISC complex may activate the type-1 pathway in a manner similar to that of the endosomal FAS-DISC complex in type-1 cells (56) (Fig. 7*B*). The endosomal DISC can then be released from the receptor to accumulate as cytosolic DISC or shunted down the endocytic degradation pathway (Fig. 7*B*). We propose that only the cytosolic DISC is competent in cleaving Bid. We propose that the majority of activated caspase-8 is lost through endocytic trafficking in *Rb-MI* cells, thus causing the lack of cytosolic IETDase activity and the defect in Bid cleavage. Consistent with this notion is the finding that pharmacological or genetic ablation of the V-ATPase can restore cytosolic IETDase and Bid cleavage in *Rb-MI* cells. Inhibition of V-ATPase prevents endosomal fusion with multivesicular bodies and lysosome as well as endosomal degradation (39, 57). The rescuing of IETDase or Bid cleavage was not observed with drugs that raise the intracellular pH (NH$_4$Cl, FCCP), inhibit autophagy (3-MA), or inhibit cathepsins (benzyloxycarbonyl-FF-fmk).

tion with TNF to induce cell death.

We have previously shown that thymocytes from Abl- or p73-deficient mice are resistant to TNF-induced apoptosis (31). With Abl- or p73-deficient mouse fibroblasts, TNF/CHX-induced apoptosis was not abolished; nevertheless, reintroduction of Abl or p73 could enhance the death response in these knock-out cells by stimulating cytochrome *c* release (31). Although Abl enhances TNF/CHX-induced fibroblast cell death, we found that the ectopic activation of Abl tyrosine kinase through inducible dimerization (61) in *Rb-MI* cells did not rescue the hTNF/CHX-induced IETDase activity (supplemental Fig. 3). However, the ectopic activation of the same dimerizable Abl kinase could stimulate IETDase in hTNF (without cycloheximide)-treated p21E cells, which lack p21Cip1 and express the adenoviral E1A protein (supplemental Fig. 3). Furthermore, siRNA-mediated knockdown of Abl did not interfere with hTNF/CHX-induced IETDase activity in *Rb-wt* cells (supplemental Fig. 3). Whereas Abl contributes to TNF-induced type-2 apoptosis, results from this study suggest
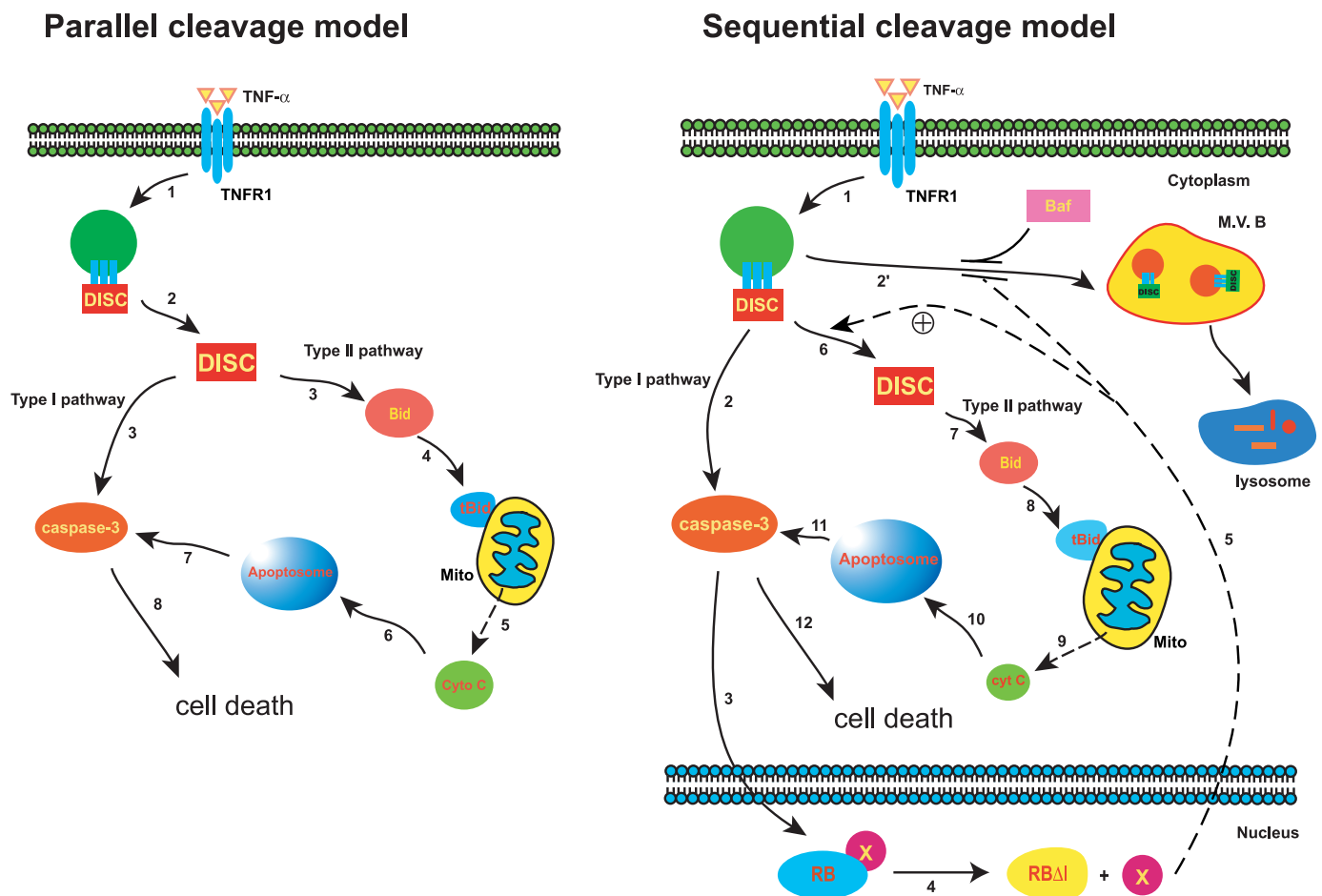
Parallel cleavage model

Sequential cleavage model

FIGURE 7. **Parallel *versus* sequential cleavage in extrinsic apoptotic pathways.** The current model of extrinsic apoptosis suggests parallel cleavage of substrates in the type-1 and the type-2 pathways by receptor-activated DISC. This model cannot explain our finding that Rb cleavage is required for Bid cleavage. We propose a sequential cleavage model, in which Rb is cleaved through the type-1 pathway, and its cleavage is a prerequisite for DISC to cleave Bid. In *Rb-MI* cells where Rb cannot be cleaved, the endosomal TNFR1-DISC complex is lost through V-ATPase-dependent endocytic trafficking. Our data suggest that Rb cleavage may cause the release of a nuclear factor that either blocks endosomal trafficking of TNFR1-DISC or stimulates DISC dissociation from the endosomal-TNFR1 to allow for Bid cleavage. The sequential cleavage model can explain why Rb cleavage is not required for TNF-induced apoptosis in type-1 cells. Rb cleavage may serve as a nuclear checkpoint for TNF-induced type-2 apoptosis.

that the blockade of Bid cleavage in *Rb-MI* cells is mediated through Abl-independent mechanisms.

We considered two possibilities for how Rb cleavage might stimulate caspase-8-dependent Bid cleavage. In the first scenario, the cleaved products (Rb-ΔI and/or the C-terminal 41-amino acid peptide) exert a positive effect on caspase-8 and Bid cleavage. In the second scenario, cleavage of Rb causes the release of a factor that stimulates the cytosolic accumulation of caspase-8, thus leading to Bid cleavage. The first scenario that Rb fragments directly activate caspase-8 or Bid cleavage is inconsistent with the result that knockdown of Rb-MI rescued cytosolic caspase-8 activity and Bid cleavage. Furthermore, knockdown of Rb-wt did not affect hTNF/CHX-induced caspase-8 activation or Bid cleavage, suggesting that Rb fragments are not required for Bid cleavage. Although we currently favor the second scenario (*i.e.* Rb cleavage causes the release of a factor (X in Fig. 7*B*) to stimulate Bid cleavage), we do not know the identity of such a factor. A previous report has shown that Rb-ΔI loses the ability to bind MDM2 (62). There is considerable evidence in the literature that MDM2 functions as an inhibitor of apoptosis (63), thus

inconsistent with MDM2 being an activator of the TNF-induced type-2 apoptotic pathway. Identification of the mechanism by which Rb-MI blocks Bid cleavage awaits further investigation.

Rb Cleavage as a Nuclear Checkpoint for TNF-induced Type-2 Apoptosis—The sequential model depicted in Fig. 7*B* suggests that cleavage of Rb may serve as a nuclear checkpoint for the activation of the type-2 apoptotic pathway by TNF. Previous studies have suggested that hyperphosphorylated Rb is more resistant to caspase cleavage (59, 64). If so, Rb cleavage is less likely to occur in $S/G_2/M$ phase cells that contain hyperphosphorylated Rb. Since TNF activates NF-κB, which promotes cell growth and survival, the Rb cleavage checkpoint may help to prevent the activation of the type-2 apoptotic pathway during TNF-stimulated cell proliferation. We have found that DSS induced colonic apoptosis to occur preferentially in the differentiated and nonproliferating epithelial cells, and it is this population of cells that are protected from apoptosis in the $Rb^{MI/MI}$ mice. The status of the Rb protein (*i.e.* phosphorylation *versus* degradation) may therefore regulate the proliferative *versus* apoptotic response to TNF.

REFERENCES

1. Karin, M., and Greten, F. R. (2005) *Nat. Rev. Immunol.* **5,** 749–759
2. Pikarsky, E., Porat, R. M., Stein, I., Abramovitch, R., Amit, S., Kasem, S., Gutkovich-Pyest, E., Urieli-Shoval, S., Galun, E., and Ben-Neriah, Y. (2004) *Nature* **431,** 461–466
3. Balkwill, F., and Coussens, L. M. (2004) *Nature* **431,** 405–406
4. Chen, G., and Goeddel, D. V. (2002) *Science* **296,** 1634–1635
5. Locksley, R. M., Killeen, N., and Lenardo, M. J. (2001) *Cell* **104,** 487–501
6. Ashkenazi, A. (2002) *Nat. Rev. Cancer* **2,** 420–430
7. Park, S.-M., Schickel, R., and Peter, M. E. (2005) *Curr. Opin. Cell Biol.* **17,** 610–616
8. Garg, A. K., and Aggarwal, B. B. (2002) *Mol. Immunol.* **39,** 509–517
9. Festjens, N., Vanden Berghe, T., and Vandenabeele, P. (2006) *Biochim. Biophys. Acta* **1757,** 1371–1387
10. Kim, Y. S., Morgan, M. J., Choksi, S., and Liu, Z. G. (2007) *Mol. Cell* **26,** 675–687
11. Kamata, H., Honda, S., Maeda, S., Chang, L., Hirata, H., and Karin, M. (2005) *Cell* **120,** 649–661
12. Kreuz, S., Siegmund, D., Scheurich, P., and Wajant, H. (2001) *Mol. Cell Biol.* **21,** 3964–3973
13. Beg, A. A., and Baltimore, D. (1996) *Science* **274,** 782–784
14. Micheau, O., Lens, S., Gaide, O., Alevizopoulos, K., and Tschopp, J. (2001) *Mol. Cell Biol.* **21,** 5299–5305
15. Dumitru, C. D., Ceci, J. D., Tsatsanis, C., Kontoyiannis, D., Stamatakis, K., Lin, J. H., Patriotis, C., Jenkins, N. A., Copeland, N. G., Kollias, G., and Tsichlis, P. N. (2000) *Cell* **103,** 1071–1083
16. Schneider-Brachert, W., Tchikov, V., Neumeyer, J., Jakob, M., Winoto-Morbach, S., Held-Feindt, J., Heinrich, M., Merkel, O., Ehrenschwender, M., and Adam, D. (2004) *Immunity* **21,** 415–428
17. Schneider-Brachert, W., Tchikov, V., Merkel, O., Jakob, M., Hallas, C., Kruse, M.-L., Groitl, P., Lehn, A., Hildt, E., Held-Feindt, J., Dobner, T., Kabelitz, D., Kronke, M., and Schutze, S. (2006) *J. Clin. Invest.* **116,** 2901–2913
18. Micheau, O., and Tschopp, J. (2003) *Cell* **114,** 181–190
19. Harper, N., Hughes, M., MacFarlane, M., and Cohen, G. M. (2003) *J. Biol. Chem.* **278,** 25534–25541
20. Welch, P. J., and Wang, J. Y. (1993) *Cell* **75,** 779–790
21. Welch, P. J., and Wang, J. Y. (1995) *Genes Dev.* **9,** 31–46
22. Lee, J. O., Russo, A. A., and Pavletich, N. P. (1998) *Nature* **391,** 859–865
23. Rubin, S. M., Gall, A. L., Zheng, N., and Pavletich, N. P. (2005) *Cell* **123,** 1093–1106
24. Heinen, C. D., Goss, K. H., Cornelius, J. R., Babcock, G. F., Knudsen, E. S., Kowalik, T., and Groden, J. (2002) *Gastroenterology* **123,** 751–763
25. Knudsen, E. S., and Wang, J. Y. J. (1996) *J. Biol. Chem.* **271,** 8313–8320
26. Janicke, R. U., Walker, P. A., Lin, X. Y., and Porter, A. G. (1996) *EMBO J.* **15,** 6969–6978
27. Natoli, G., Costanzo, A., Ianni, A., Templeton, D. J., Woodgett, J. R., Balsano, C., and Levrero, M. (1997) *Science* **275,** 200–203
28. Tan, X., and Wang, J. Y. (1998) *Trends Cell Biol.* **8,** 116–120
29. Hiebert, S. W., Chellappan, S. P., Horowitz, J. M., and Nevins, J. R. (1992) *Genes Dev.* **6,** 177–185
30. Chau, B. N., Borges, H. L., Chen, T. T., Masselli, A., Hunton, I. C., and Wang, J. Y. (2002) *Nat. Cell Biol.* **4,** 757–765
31. Chau, B. N., Chen, T. T., Wan, Y. Y., DeGregori, J., and Wang, J. Y. (2004) *Mol. Cell Biol.* **24,** 4438–4447
32. Wajant, H. (2002) *Science* **296,** 1635–1636
33. Scaffidi, C., Fulda, S., Srinivasan, A., Friesen, C., Li, F., Tomaselli, K. J., Debatin, K. M., Krammer, P. H., and Peter, M. E. (1998) *EMBO J.* **17,** 1675–1687
34. Li, H., Zhu, H., Xu, C. J., and Yuan, J. (1998) *Cell* **94,** 491–501
35. Beyenbach, K. W., and Wieczorek, H. (2006) *J. Exp. Biol.* **209,** 577–589
36. Inoue, T., Wang, Y., Jefferies, K., Qi, J., Hinton, A., and Forgac, M. (2005) *J. Bioenerg. Biomembr.* **37,** 393–398
37. Sun-Wada, G.-H., Wada, Y., and Futai, M. (2004) *Biochim. Biophys. Acta* **1658,** 106–114
38. Johnson, L. S., Dunn, K. W., Pytowski, B., and McGraw, T. E. (1993) *Mol. Biol. Cell* **4,** 1251–1266
39. Hurtado-Lorenzo, A., Skinner, M., El Annan, J., Futai, M., Sun-Wada, G. H., Bourgoin, S., Casanova, J., Wildeman, A., Bechoua, S., and Ausiello, D. A. (2006) *Nat. Cell Biol.* **8,** 124–136
40. Varfolomeev, E. E., Schuchmann, M., Luria, V., Chiannilkulchai, N., Beckmann, J. S., Mett, I. L., Rebrikov, D., Brodianski, V. M., Kemper, O. C., Kollet, O., Lapidot, T., Soffer, D., Sobe, T., Avraham, K. B., Goncharov, T., Holtmann, H., Lonai, P., and Wallach, D. (1998) *Immunity* **9,** 267–276
41. Tu, S., McStay, G. P., Boucher, L. M., Mak, T., Beere, H. M., and Green, D. R. (2006) *Nat. Cell Biol.* **8,** 72–77
42. Trombetta, E. S., Ebersold, M., Garrett, W., Pypaert, M., and Mellman, I. (2003) *Science* **299,** 1400–1403
43. Martin, D. A., Siegel, R. M., Zheng, L., and Lenardo, M. J. (1998) *J. Biol. Chem.* **273,** 4345–4349
44. Luo, X., Budihardjo, I., Zou, H., Slaughter, C., and Wang, X. (1998) *Cell* **94,** 481–490
45. Kuwana, T., Mackey, M. R., Perkins, G., Ellisman, M. H., Latterich, M., Schneiter, R., Green, D. R., and Newmeyer, D. D. (2002) *Cell* **111,** 331–342
46. Boatright, K. M., Renatus, M., Scott, F. L., Sperandio, S., Shin, H., Pedersen, I. M., Ricci, J. E., Edris, W. A., Sutherlin, D. P., and Green, D. R. (2003) *Mol. Cell* **11,** 529–541
47. Boatright, K. M., and Salvesen, G. S. (2003) *Curr. Opin. Cell Biol.* **15,** 725–731
48. Kang, T. B., Ben-Moshe, T., Varfolomeev, E. E., Pewzner-Jung, Y., Yogev, N., Jurewicz, A., Waisman, A., Brenner, O., Haffner, R., and Gustafsson, E. (2004) *J. Immunol.* **173,** 2976–2984
49. Helfer, B., Boswell, B. C., Finlay, D., Cipres, A., Vuori, K., Bong Kang, T., Wallach, D., Dorfleutner, A., Lahti, J. M., Flynn, D. C., and Frisch, S. M. (2006) *Cancer Res.* **66,** 4273–4278
50. Ohkuma, S., and Poole, B. (1978) *Proc. Natl. Acad. Sci. U. S. A.* **75,** 3327–3331
51. Lin, Y., Choksi, S., Shen, H. M., Yang, Q. F., Hur, G. M., Kim, Y. S., Tran, J. H., Nedospasov, S. A., and Liu, Z. (2004) *J. Biol. Chem.* **279,** 10822–10828
52. Borges, H. L., Bird, J., Wasson, K., Cardiff, R. D., Varki, N., Eckmann, L., and Wang, J. Y. J. (2005) *Proc. Natl. Acad. Sci. U. S. A.* **102,** 15587–15592
53. Li, K., Li, Y., Shelton, J. M., Richardson, J. A., Spencer, E., Chen, Z. J., Wang, X., and Williams, R. S. (2000) *Cell* **101,** 389–399
54. Ruffolo, S. C., Breckenridge, D. G., Nguyen, M., Goping, I. S., Gross, A., Korsmeyer, S. J., Li, H., Yuan, J., and Shore, G. C. (2000) *Cell Death Differ.* **7,** 1101–1108
55. Kohlhaas, S. L., Craxton, A., Sun, X. M., Pinkoski, M. J., and Cohen, G. M. (2007) *J. Biol. Chem.* **282,** 12831–12841
56. Lee, K. H., Feig, C., Tchikov, V., Schickel, R., Hallas, C., Schutze, S., Peter, M. E., and Chan, A. C. (2006) *EMBO J.* **25,** 1009–1023
57. Clague, M. J., Urbe, S., Aniento, F., and Gruenberg, J. (1994) *J. Biol. Chem.* **269,** 21–24
58. Chau, B. N., and Wang, J. Y. (2003) *Nat. Rev. Cancer* **3,** 130–138
59. Tan, X., Martin, S. J., Green, D. R., and Wang, J. Y. J. (1997) *J. Biol. Chem.* **272,** 9613–9616
60. Whitaker, L. L., Su, H., Baskaran, R., Knudsen, E. S., and Wang, J. Y. (1998) *Mol. Cell Biol.* **18,** 4032–4042
61. Vella, V., Zhu, J., Frasca, F., Li, C. Y., Vigneri, P., Vigneri, R., and Wang, J. Y. (2003) *J. Biol. Chem.* **278,** 25151–25157
62. Xiao, Z. X., Chen, J., Levine, A. J., Modjtahedi, N., Xing, J., Sellers, W. R., and Livingston, D. M. (1995) *Nature* **375,** 694–698
63. Vargas, D. A., Takahashi, S., and Ronai, Z. (2003) *Adv. Cancer Res.* **89,** 1–34
64. Fattman, C. L., An, B., and Dou, Q. P. (1997) *J. Cell. Biochem.* **67,** 399–408